Foot and Ankle Surgery 22 (2016) 158–163

Contents lists available at ScienceDirect

Foot and Ankle Surgery

journal homepage: www.elsevier.com/locate/fas

Comparison of modern locked plating and antiglide plating for fixation of osteoporotic distal fibular fractures

Paul J. Switaj MD[a,*], Robert J. Wetzel MD[a], Neel P. Jain MD[b], Brian M. Weatherford MD[c], Yupeng Ren PhD[d], Li-Qun Zhang PhD[e], Bradley R. Merk MD[a]

[a] Department of Orthopaedic Surgery, Northwestern University, Chicago, IL, USA
[b] Department of Orthopaedic Surgery, Franciscan Alliance, Michigan City, IN, USA
[c] Orthopaedic Associates of Michigan, Grand Rapids, MI, USA
[d] Rehabilitation Institute of Chicago, Chicago, IL, USA
[e] Rehabilitation Institute of Chicago, Chicago, IL, USA

ARTICLE INFO

Article history:
Received 15 March 2015
Received in revised form 21 May 2015
Accepted 24 June 2015

Keywords:
Fibula
Fixation
Osteoporosis
Antiglide
Locked plating

ABSTRACT

Background: Fractures in osteoporotic patients can be difficult to treat because of poor bone quality and inability to gain screw purchase. The purpose of this study is to compare modern lateral periarticular distal fibula locked plating to antiglide plating in the setting of an osteoporotic, unstable distal fibula fracture.

Methods: AO/OTA 44-B2 distal fibula fractures were created in sixteen paired fresh frozen cadaveric ankles and fixed with a lateral locking plate and an independent lag screw or an antiglide plate with a lag screw through the plate. The specimens underwent stiffness, cyclic loading, and load to failure testing. The energy absorbed until failure, torque to failure, construct stiffness, angle at failure, and energy at failure was recorded.

Results: The lateral locking construct had a higher torque to failure ($p = 0.02$) and construct stiffness ($p = 0.04$). The locking construct showed a trend toward increased angle at failure, but did not reach statistical significance ($p = 0.07$). Seven of the eight lateral locking plate specimens failed through the distal locking screws, while the antiglide plating construct failed with pullout of the distal screws and displacement of the fracture in six of the eight specimens.

Conclusion: In our study, the newly designed distal fibula periarticular locking plate with increased distal fixation is biomechanically stronger than a non-locking one third tubular plate applied in antiglide fashion for the treatment of AO/OTA 44-B2 osteoporotic distal fibula fractures.

Level of evidence: V: This is an ex-vivo study performed on cadavers and is not a study performed on live patients. Therefore, this is considered Level V evidence.

1. Introduction

An unstable ankle fracture has been shown to be an indication for open reduction and internal fixation in order to lower the risk of posttraumatic arthritis secondary to abnormal loading [1]. Overall, this has been associated with good surgical outcomes [2]. When occurring in osteoporotic bone, these fractures can be difficult to treat because of poor bone quality and inability to gain screw purchase [1].

There have been a variety of implants described to treat distal fibula fractures, including lateral non-locking plates, lateral locking plates, and posterolateral antiglide plating. Lateral application of a plate on the distal fibula is typically in neutralization mode after the placement of a lag screw across the fracture site. On the posterolateral surface, the plate is applied directly over the proximal apex of the fracture, in antiglide fashion. Lag compression can be achieved by inserting a lag screw through the plate in a posterior-to-anterior direction. Given these options, it is important for the treating surgeon to consider methods of fixation that will maximize the stability of anatomic reduction while minimizing complications.

Locked plating has been used in the treatment of metaphyseal fractures when there is a short distal end segment that limits the options for screw fixation, such as in the distal fibula. There is some

* Corresponding author at: Department of Orthopaedic Surgery, Northwestern University Feinberg School of Medicine, 676 N St. Clair, St. Suite 1350, Chicago, IL 60611, USA. Tel.: +1 312 926 4444; fax: +1 312 916 4643.
E-mail address: paul.switaj@gmail.com (P.J. SwitajMD).

http://dx.doi.org/10.1016/j.fas.2015.06.007
1268-7731/

evidence that the biomechanical effectiveness of lateral locking plate fixation is independent of bone mineral density (BMD) while non-locking lateral plate fixation is dependent on BMD [3]. However, when compared to antiglide plates in a cadaveric model that was tested in torsion, Minihane et al. suggests that lateral locking plates are biomechanically inferior in the setting of osteoporotic distal fibula fractures [4]. Additionally, antiglide plating has demonstrated its effectiveness in the setting of osteoporotic distal fibula fractures [5].

Antiglide plating has long been associated with tendon irritation and high rates of hardware removal [6]. Prior studies demonstrating the superior function of posterolateral non-locking antiglide fixation, such as that by Minihane et al., utilized a locking one third tubular plate in their comparison, which only provided two points of fixation in the distal segment [4]. However, more recently Zahn et al. have shown that anatomically contoured distal fibular locking plates are biomechanically superior to non-locking lateral plates in a cadaveric model [7]. By increasing the distal fixation with modern locked plating, this may decrease the rate of peroneal irritation while providing a construct that may exhibit biomechanical superiority, especially in patients with poor bone quality.

The purpose of this study was to evaluate an anatomically contoured distal fibular lateral locking plate that utilizes increased distal fixation and compare it to non-locked antiglide plating in unstable, osteoporotic distal fibula fractures. Prior to the study, we believed that there would be no difference in the construct stiffness, failure strength, and energy absorbed in the failure test between the lateral periarticular distal fibula locked plating to the antiglide plating.

2. Materials and methods

2.1. Specimen preparation

Eight paired (sixteen total) fresh frozen cadaveric ankle specimens were obtained from the mid-tibia to the foot and stored in a freezer at −20 °C. All specimens were Caucasian females over the age of 75. The average age of the specimens was 86 years old (range 75–94). Prior to dissection and experimentation, all specimens were thawed for 24 h at room temperature in a cooler. None of the specimens had any prior ankle surgery or deformity. BMD values were obtained for all specimens using dual-energy X-ray absorptiometry scans of the calcaneus (Hologic Explorer, Bedford, MA).

Preparation of the specimens started with dissection of the proximal 5 cm to expose the tibia and fibula. The fibula was secured to the tibia with a 3.5 mm fully threaded cortical screw, maintaining the interosseous distance between the tibia and fibula. This is consistent with prior studies done at our institution, and could find no evidence in prior biomechanical literature to suggest that this affected our ankle stability. Next, the fibula was resected proximal to the screw placement in order to allow placement of the tibia into the apparatus. An ankle fracture was then simulated to reproduce a Weber B or Supination-External Rotation (SER) IV deltoid equivalent [8] type of ankle fracture (AO/OTA 44-B2). The distal fibula was exposed, and the skin and subcutaneous tissues were removed to provide adequate exposure. The anterior and posterior tibiofibular ligaments were identified and sectioned. Next, the medial skin and subcutaneous tissues were removed, and the deltoid ligament was identified and sectioned. Lastly, a distal fibula fracture was simulated with the use of an oscillating saw to create an oblique osteotomy. The osteotomy started distally and anteriorly at the level of the tibiotalar joint, and was directed proximally and posteriorly at an angle of 60° to simulate a typical fracture orientation (Fig. 1A).

Fig. 1. (A) Exposure and preparation of distal fibula for testing; (B) Fixation with the antiglide plate and lag screw through the plate; (C) Fixation with the lateral periarticular locking plate and independent lag screw.

Each pair of specimens was then randomized to one construct on one side of the ankle using the posterolateral antiglide plate and the contralateral side using the lateral locking plate.

2.2. Surgical technique

All cadaveric surgery work was done by a senior level orthopaedic resident and the fractures were anatomically reduced and fixed in the following, standardized manner. For the antiglide plating group, a 5-hole one-third tubular plate (Synthes, Paoli, PA) was used. The plate was placed posterolaterally and secured with two 3.5 mm bicortical screws proximal to the fracture, a 3.5 mm bicortical lag screw placed through the plate starting distal to the fracture, and a unicortical 4.0 mm fully threaded cancellous screw in the most distal hole of the plate (Fig. 1B) [9]. These plates were minimally contoured to ensure an antiglide/buttress effect. For the lateral locking plate group, a six hole VariAx ® (Stryker, Mahwah,

NJ) plate was used. The fracture was first secured with a 3.5 mm bicortical lag screw placed outside of the plate starting proximal to the fracture. Next, the plate was positioned appropriately and fixed with two proximal 3.5 mm bicortical screws. The plates were then fixed with four 3.5 mm diameter, 14 mm long unicortical locking screws placed distal to the fracture. These were placed by hand until the screw heads were visualized to appropriately engage into the threads into the plate, without stripping the screw heads (Fig. 1C).

2.3. Biomechanical testing

After appropriate fixation, the specimens were then loaded into a custom designed, multi-axial biomechanical apparatus which allowed a controlled rate of rotation and was able to measure angular displacement and torque with the use of a servomotor, reaction torque sensor, and motor encoder. The apparatus and subsequent protocol had previously been used in a similar biomechanical study at the same institution [4].

The tibia was secured into an aluminum cylinder using multiple rows of sharp tipped bolts [4,10–12] screwed radially to hold the tibia securely. This aluminum cylinder was secured to an X–Y platform that allowed the aluminum cylinder and the tibia to slide in the anteroposterior and mediolateral directions. The tibia was secured in the aluminum cylinder assuring proper axial orientation in the coronal and sagittal planes. Additionally, the foot was secured in a footplate with two metal straps over the metatarsals and two bolts through the calcaneus. A neutral rotation point was set using the angle between the transmalleolar axis and the second metatarsal, which was measured prior to dissection. The foot was positioned in the footplate to 25° of supination and 10° of dorsiflexion using wedged blocks, and a 600 N load was placed over the upper sliding platform to simulate the body weight of an elderly, osteoporotic individual (Fig. 2).

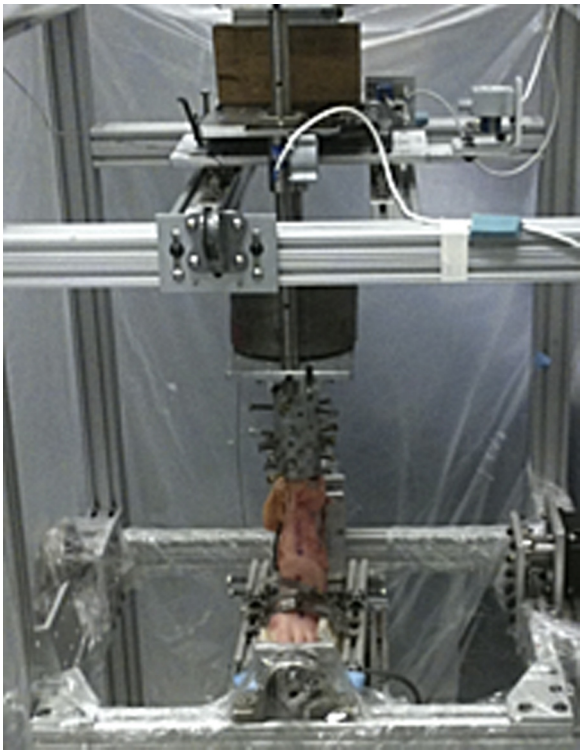

Fig. 2. Setup of specimen in apparatus. Note 600 N axial load, alignment of specimen, with freedom in the coronal and sagittal planes.

The specimen testing was divided into four phases: pre-cyclic loading stiffness, cyclic loading, post-cyclic loading stiffness, and torque to failure. For the pre-cyclic loading stiffness testing, the 600 N load and initial foot position was maintained throughout and the specimen was cycled at a rate of 10°/s to a torque limit of 5 Nm in external and internal rotation [13]. The specimen was then cyclically loaded at a rate of 30°/s for 1000 cycles from a neutral position of rotation to a torque limit of 5 Nm in external rotation. This was followed by a repeat stiffness test similar to the pre-cyclic loading stiffness. The final test involved a torque to failure test where the specimens were externally rotated at a rate of 60°/s to an angular displacement of 90°. The failure point was defined as a sudden drop in resistance torque in the torque–angle curve during the failure test that correlated to a visual failure of the construct during controlled external rotation.

2.4. Data analysis

The data were then analyzed using custom programs in Matlab (Mathworks™, Natick, MA). The external rotation laxity and range of motion was determined as the joint position change at 5 Nm of external rotation torque. The total energy absorbed until failure for each construct was calculated for all specimens. This was determined by calculating the area under the torque–angle curve for the torque to failure test.

For the specimens that failed during cyclical loading, the point of failure was determined by a sudden change in angular displacement for the 5 Nm torque applied. Additionally, failure was confirmed with visual observation during testing. For the specimens that completed the final phase of testing, the torque to failure, construct stiffness, and angular displacement at failure were recorded. Construct stiffness was calculated by using the slope of the linear portion of the torque to angular displacement curve. Torque to failure and angular displacement at failure were determined by a sudden drop in the resistance torque of the torque–angle curve (Fig. 3). The initial shallow gradient of the curve is likely a result early soft tissue tensioning of the remaining intact structures.

Analysis of variance (ANOVA) with repeated measures was used to compare the laxity, range of motion and stiffness across the pre- and post-cyclic loading conditions and between the two methods of fixation. Paired student *t*-tests were used to compare the BMD, failure torque, failure energy, angle at failure, and stiffness during failure tests between the two methods of fixation. The level of statistical significance was set at 0.05.

3. Results

3.1. Bone mineral density

The BMD of the lateral locking plate specimens was not different from the BMD of the antiglide plate specimens (0.240 ± 0.117 g/cm^2 vs. 0.241 ± 0.123 g/cm^2, $p = 0.50$). This finding confirms our paired specimen experimental setup provided equivalent bone quality for both plating groups. Using previously established criteria, six out of the eight paired specimens would be considered osteoporotic [14,15]. The BMD of the specimens that failed prior to the final phase of testing was not statistically different from those that underwent the load to failure test ($p = 0.18$).

3.2. External rotation stiffness

The stiffness of the specimens was determined based on pre-cyclic loading and post-cyclic loading testing. The pre-cyclic loading stiffness of the lateral locking plate was not different from the antiglide plate (0.26 ± 0.16 Nm/degree vs.

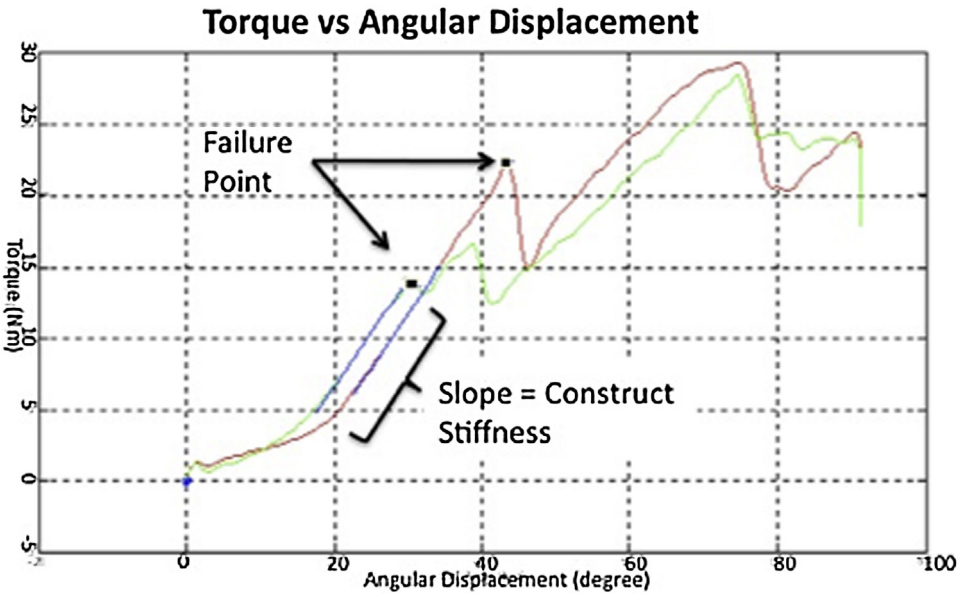

Fig. 3. Torque–angular displacement curve of a load-to-failure test. The curve associated with the greater torque to failure corresponds to the lateral locking plate (red). The lower failure point corresponds to the antiglide plate (green). The slope of the linear portion of the curves (blue lines) corresponds the construct stiffness. The area under the linear section of graph represents the energy absorbed (For interpretation of the color information in this figure legend, the reader is referred to the web version of the article.).

0.25 ± 0.13 Nm/degree, $p = 0.32$). The post-cyclic loading stiffness was determined for the ten specimens that remained intact for this phase of testing. As expected, for each plate construct the stiffness decreased after cyclical loading. The locking plate construct had higher construct stiffness at failure than the antiglide plating construct (0.67 ± 0.21 Nm/degree vs. 0.52 ± 0.26 Nm/degree, $p = 0.04$) (Table 1).

3.3. Failure of specimens

When comparing all specimens, the energy absorbed for the lateral locking plate construct throughout the cyclic loading was significantly greater than the antiglide plating construct (29515 ± 11958 Nm/degree vs. 24968 ± 13190 Nm/degree, $p = 0.03$). The locking plate construct had a significantly higher torque to failure than the antiglide plating construct (16.5 ± 7.61 Nm vs. 10.54 ± 6.42 Nm, $p = 0.02$). The energy spent on failure was about 170% higher for the lateral locking plate compared to the antiglide plate (426 ± 164 Nm/degree vs. 248 ± 102 Nm/degree, $p = 0.048$). There was trend towards a higher angle of failure in the locking plate construct group than the antiglide plating construct, but this did not reach statistical significance (42 ± 13° vs. 32 ± 9.2°, $p = 0.07$) (Table 2).

Of the sixteen specimens, six constructs failed prior to reaching the final stage of testing. Two specimens failed in the pre-cyclic loading stiffness testing (both antiglide plating constructs), four specimens failed during cyclic loading (two from each construct group), and the remaining ten specimens completed torque to failure testing. It should be noted that the two locking plate specimens that failed had their respective matched pairs also fail during cyclic loading in the antiglide plating group. These lateral locking plate constructs failed at a later point than their matched counterpart (330 vs. 2 cycles, 144 vs. 5 cycles). The early failures within the antiglide plating group implies that their torque to failure was around the torque limit set for cyclical loading which was 5 Nm. The early failures of the locking plate specimens that failed during cyclical loading also implies a torque limit of around 5 Nm, however they were able to withstand a greater number of cycles prior to failing (Table 2).

Lastly, all specimens were inspected for their modes of failure. The antiglide plating construct failed with pullout of the distal screws and displacement of the fracture in six of the eight

Table 1
External rotation stiffness data for each plate construct.

External rotation stiffness (Nm/degree)	Antiglide plate	Locked plate	*p*-Value
Pre-cyclic loading	0.25 ± 0.13	0.26 ± 0.16	0.3
Post-cyclic loading	0.14 ± 0.09	0.16 ± 0.10	0.3
At failure	0.52 ± 0.26	0.67 ± 0.21	*0.04*

Please note these numbers reflect means with 95% confidence intervals. Italicized values represent a significant difference.

Table 2
Biomechanical failure properties of specimens. Torque to failure assumed to be 5 Nm for specimens that failed prior to load to failure test.

Failure properties	Antiglide plate	Locked plate	*p*-Value
Torque to failure (Nm)	10.5 ± 6.4	16.6 ± 7.6	*0.03*
Angle at failure (Degree)	31.9 ± 9.19	41.9 ± 13.5	0.07
Energy absorbed (Nm/degree)	$24.9 \times 10^3 \pm 13.2 \times 10^3$	$29.5 \times 10^3 \pm 11.9 \times 10^3$	*0.03*
Failure (# of specimens)			
Pre-cyclic stiffness test	2	0	
Cyclic loading	2	2	
# of cycles	2, 5	330, 144	
Load to failure	4	6	

Please note these numbers reflect means with 95% confidence intervals. Italicized values represent a significant difference.

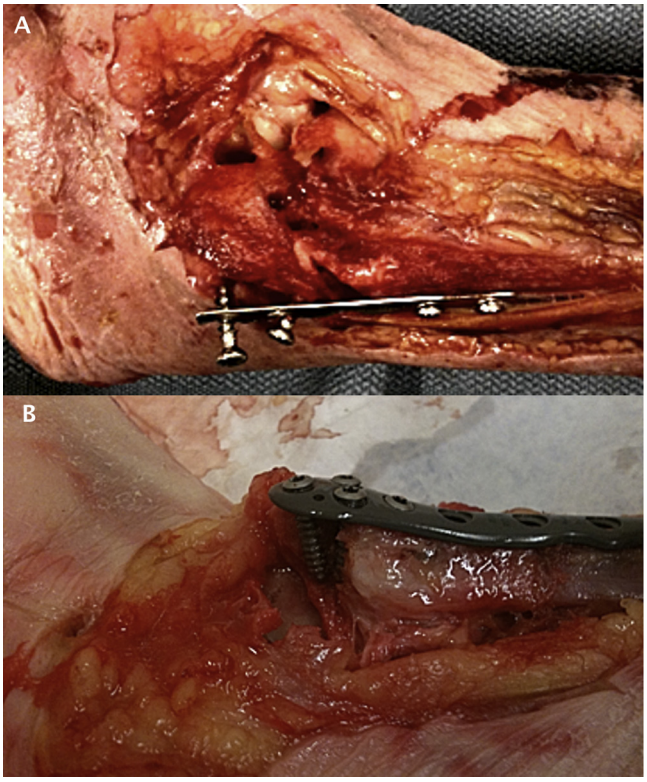

Fig. 4. (A) Failure mode of lateral locking plate constructs. Note intact nature of fracture with fragmentation of distal segment around distal locking screw cluster; (B) Failure mode of antiglide plate construct. Note pullout of distal screws with displacement of fracture.

specimens (Fig. 4A). In the remaining two specimens, there was pullout of the distal screws with fragmentation of the distal fragment. Seven of the eight lateral locking plate specimens failed through the distal locking screws. The fracture itself remained intact with fragmentation of the distal fibula through the distal cluster of screws (Fig. 4B). The remaining specimen in this group failed with pullout of the distal locking screws and displacement of the fracture.

4. Discussion

Fixation of distal fibula fractures in osteoporotic bone is a surgical challenge. Given the increasing elderly population, surgeons are more likely to confront osteoporotic ankle fractures. In the elderly, surgical intervention has been proven to be superior to conservative management in unstable ankle fractures [2]. There have been numerous studies evaluating different fixation techniques in osteoporotic ankle fractures [16–18]. To our knowledge, this is the first study suggest that a lateral locked plating construct has a biomechanical advantage over posterolateral non-locked antiglide plating.

Two common fixation constructs used for distal fibula fractures include antiglide plating and lateral plating. Antiglide plating was first described by Brunner and Weber in 1982 where they described proper application techniques and demonstrated how it avoids certain complications related to lateral plating [9]. A variety of studies have assessed the outcomes of antiglide plates [6,19–21]. These studies have demonstrated relatively low complication rates with high patient satisfaction. However, a recent study by Weber and Krause demonstrated a relatively high complication rate with posterolateral antiglide plating [6]. The hardware removal rate was 43%, with 30% of these patients having peroneal tendon lesions. The lateral plate should theoretically avoid these complications.

There have been few studies comparing lateral locked or non-locked plating to antiglide plating. Most recently, Minihane et al. performed a cadaveric study and found the antiglide plate to be biomechanically superior to a one third tubular locking plate in osteoporotic bone [4]. Schaffer and Manoli also performed a cadaveric study and found the antiglide plate biomechanically superior to a traditional lateral plating technique [22]. Lamontagne et al. evaluated the clinical results of antiglide plating to lateral non-locked plating and found no statistical difference in patient outcomes or complications rates [23].

Locked plating technology has been popularized by its ability to achieve increased fixation in osteoporotic bone [24–26]. Kim et al. performed a biomechanical cadaveric study comparing locked lateral plates to traditional lateral plates in osteoporotic bone [3]. There was no statistical difference shown between the two constructs, however the locked plating strength was shown to be independent of bone mineral density. Minihane et al. demonstrated superiority of antiglide plating to lateral locked plating [4], however, in the lateral locked plate group, there were only two screws placed distal to the fracture. Since that study, newer periarticular plates have been developed, and Zahn et al. has described an anatomically contoured laterally based periarticular locking plate with four 2.7 mm distal locking screws to be biomechanically stronger than a non-locking laterally based anatomically contoured plate [7]. The impetus for the locking plate used in our study was to provide increased fixation in the distal fragment and compare it to antiglide plating. The data in this study, and in the study by Zahn et al. infers that the construct is biomechanically strengthened with the increased number of distal locking screws [7]. This increased construct stiffness may provide superior stability at the fracture site during healing, but we do not believe it would change the long-term biomechanics at the ankle joint after fracture union.

While our results seem to agree with Zahn et al. [7] it should be noted that we also included cyclic loading in our failure testing, something that is lacking from their work. This is more clinically relevant, since the required loads to failure are most likely higher than those seen in a typical postoperative course [9]. Four of the eight antiglide specimens and two of the eight locked plates failed prior to reaching the load to failure test. Given the early failures were likely related to the threshold in those specimens being close to the cyclical loading torque, we assumed the torque to failure of these specimens to be 5 Nm. To further compare all specimens, we also calculated the energy absorbed, which was found to be greater in the lateral locking plate construct.

Interestingly, a majority of the lateral locking plate constructs failed catastrophically around the distal locking screws. The fracture itself remained relatively nondisplaced with fragmentation of the distal segment. A potential disadvantage of the increased number of distal locking screws is weakening of the bone, and in the setting of preexisting weakened osteoporotic bone, creating more bony defects with the screw creates an area predisposed to fracture. With this in mind, we still found the amount of torque that led to this failure mode was higher than the amount of torque required to fail the antiglide plating constructs.

This biomechanical study has some limitations. Our study utilized an osteotomy and ligament sectioning that has been used in other biomechanical studies [3–5]. However, the ability to recreate an accurate portrayal of an osteoporotic ankle fracture is difficult. While this study may not be able to fully recreate small zones of comminution often seen in these fractures, utilizing matched osteoporotic pairs allowed us to make an adequate comparison between two common fixation constructs in clinical practice. Also, given this lack of constraint in the axial, coronal, and

sagittal planes combined with the osteoporotic nature of the specimens, 600 N may have excessive for the capacity of the osteoporotic specimens. Minihane et al. [4] and Zahn et al. [7] had models that were loaded to 700 N and 800 N, respectively, but in both studies there was a higher degree of constraint. In osteoporotic model used in Zahn et al. [7], they did not section the surrounding ligaments as we did, leading to a greater deal of stability with some energy from the testing absorbed by the soft tissues. The torque limit used in our cyclic loading model was 5 Nm. Based on previous studies, this appeared to be in the mid elastic portion of the stress strain curve of the plating constructs [3]. However, fifty percent of the antiglide specimens failed prior to reaching the final stage. This supports our portrayal of a clinically relevant failure, however many of these specimens failed early in the cyclic loading process. In the future, in addition to decreasing the simulated body weight and cyclical loading torque, an increased number of specimens would increase the power of the study.

Despite these findings, because we used paired specimens, we still were able to find a difference between the two constructs even in those specimens that failed early. Finally, we also do acknowledge that in the locking plate construct also utilized a lag screw in addition to the plate. We chose to do this allow both the locking and antiglide group to achieve perpendicular compression of the osteotomy, with the antiglide group doing so through the plate itself and the locking group with an independent screw. Because the lag screw in the locking group was in an independent plane as the plate and locking screws, it may have added to the stiffness of the locking construct in its entirety. Although, we did not see any failures in the locking plate group at the level of the lag screw, but instead all failures were at the distal screw cluster. This suggests to us that intrinsic stiffness of the locking plate construct itself was likely not great affected by the addition of the lag screw.

In conclusion, this study demonstrates the lateral periarticular distal fibula locking plate to be superior to a one third tubular antiglide plate in torsional and external rotational loading in an osteoporotic, cadaveric model. Anatomically contoured distal fibula locking plates with increased points of fixation in the distal segment may provide surgeons with a stronger alternative in the setting of unstable, osteoporotic distal fibula fractures.

Conflict of interest

Dr. Merk discloses he is a consultant for Stryker, receives research support from Stryker and Synthes, and is on the Editorial Board for *The American Journal of Orthopedics*.

Disclosure

All authors were fully involved in the study and preparation of the manuscript. This material has not been accepted submitted for publication elsewhere.

Acknowledgements

The authors would like the thank Mahesh Polavarapu, BS, and Xin Guo, MS, for their assistance in the biomechanical aspects of this project.

Stryker (Mahwah, NJ) provided a grant for cadaveric specimens and implants.

References

[1] Michelson J. Fractures about the ankle. J Bone Joint Surg (Am) 1995;77(1):142–52.
[2] Ali MS, McLaren CAN, Rouholamin E, O'Connor BT. Ankle fractures in the elderly: nonoperative or operative treatment. J Orthop Trauma 1988;1(4):275–80.
[3] Kim T, Ayturk UM, Haskell A, Miclau T, Puttlitz CM. Fixation of osteoporotic distal fibula fractures: a biomechanical comparison of locking versus conventional plates. J Foot and Ankle Surg 2007;46(1):2–6.
[4] Minihane KP, Lee C, Ahn C, Zhang L-Q, Merk BR. Comparison of lateral locking plate and antiglide plate for fixation of distal fibular fractures in osteoporotic bone: a biomechanical study. J Orthop Trauma 2006;20(8):562–6.
[5] Winkler B, Weber BG, Simpson LA. The dorsal antiglide plate in the treatment of Danis–Weber Type B fractures of the distal fibula. Clin Orthop Rel Res 1990;204–9. Oct (259).
[6] Weber M, Krause F. Peroneal tendon lesions caused by antiglide plates used for fixation of lateral malleolar fractures: the effect of plate and screw position. Foot Ankle Int 2005;281–5. Apr(26).
[7] Zahn RK, Frey S, Jakubietz RG, et al. A contoured locking plate for distal fibular fractures in osteoporotic bone: a biomechanical cadaver study. Injury 2012;43(6):718–25.
[8] Lauge-Hansen N. Fractures of the ankle. II. Combined experimental-surgical and experimental-roentgenologic investigations. Arch Surg 1950;60:957–85.
[9] Brunner CF, Weber BG. The antiglide plate, special techniques in internal fixation. New York: Springer-Verlag; 1982. p. 115–33.
[10] Ho JY, Ren Y, Kelikian A, Aminian A, Charnley I, Zhang L-Q. Mid-diaphyseal fibular fractures with syndesmotic disruption: should we plate the fibula? Foot Ankle Int 2008;29:587–92.
[11] Fukuda T, Haddad SL, Ren Y, Zhang L-Q. Impact of talar component rotation on contact pressure after total ankle arthroplasty. A cadaveric study. Foot Ankle Int 2010;31(5):404–11.
[12] Haddad SL, Dedhia S, Ren Y, Rotstein J, Zhang L-Q. Deltoid ligament reconstruction: a novel technique with biomechanical analysis. Foot Ankle Int 2010;31(7):639–51.
[13] Klitzman R, Zhao H, Zhang L-Q, Strohmeyer G, Vora A. Suture-button versus screw fixation of the syndesmosis: a biomechanical analysis. Foot Ankle Int 2010;31(1):69–75.
[14] Yamada M, Ito M, Hayashi K, Nakamura T. Calcaneus as a site for assessment of bone mineral density: evaluation in cadavers and healthy volunteers. Am J Roent 1993;621–7. Sept(161).
[15] Yamada M, Ito M, Hayashi K, Ohki M, Nakamura T. Dual energy X-ray absorptiometry of the calcaneus: comparison with other techniques to assess bone density and value in predicting risk of spine fracture. Am J Roent 1994;1435–40. Dec(163).
[16] Dunn WR, Easley ME, Parks BG, Trnka HJ, Schon LC. An augmented fixation methods for distal fibular fractures in elderly patients: a biomechanical evaluation. Foot Ankle Int 2004;128–31. March(25 (3)).
[17] Koval KJ, Petraco DM, Kummer FJ, Bharam S. A new technique for complex fibula fracture fixation in the elderly: a clinical and biomechnical evaluation. J Orthop Trauma 1997;28–33. Jan(11(1)):.
[18] Pritchett JW. Rush rods versus plate osteosyntheses for unstable ankle fractures in the elderly. Orthop Rev 1993;691–6. Jun(22(6)).
[19] Ostrum RF. Posterior plating of displaced Weber B fibula fractures. J Orthop Trauma 1996;10(3):199–203.
[20] Treadwell JR, Fallat LM. The antiglide plate for the Danis–Weber Type B fibular fracture: a review of 71 cases. J Foot and Ankle Surg 1993;573–9. Nov-Dec(32(6)):.
[21] Wissing JC, van Laarhoven CJ, van der Werken C. The posterior antiglide plate for fixation of fractures of the lateral malleolus. Injury 1992;23(2):94–6.
[22] Schaffer JJ, Manoli IA. The antiglide plate for distal fibular fixation. J Bone Joint Surg (Am) 1987;69-A(4):596–604.
[23] Lamontagne J, Blachut PA, Broekhuyse HM, O'Brien PJ, Meek RN. Surgical treatment of a displaced lateral malleolus fracture: the antiglide technique versus lateral plate fixation. J Orthop Trauma 2002;16(7):498–502.
[24] Gardner MJ, Helfet DL, Lorich DG. Has locked plating completely replaced conventional plating? Am J Orthop (Belle Mead NJ) 2004;439–46. Sept(33(9)).
[25] Egol KA, Kubiak EN, Fulkerson E, Kummer FJ, Koval KJ. Biomechniacs of locked plates and screws. J Orthop Trauma 2004;18(8):488–93.
[26] Haidukewych GJ. Innovations in locked plate technology. J Am Acad Orthop Surg 2004;12:205–12.